Changes in binding of [123I]Clinde, a high-affinity translocator protein 18 kDa (TSPO) selective radioligand in a rat model of traumatic brain injury.

Donat CK, Gaber K, Meixensberger J, Brust P, Pinborg LH, Hansen HH, Mikkelsen JD

First published online: 11 March 2016

by Springer

in NeuroMolecular Medicine

Changes in binding of [^{123}I]CLINDE, a high-affinity translocator protein 18 kDa (TSPO) selective radioligand in a rat model of traumatic brain injury

Cornelius K. Donat[1*], Khaled Gaber[2], Jürgen Meixensberger[2], Peter Brust[3], Lars H. Pinborg[1], Henrik H. Hansen[1] and Jens D. Mikkelsen[1]

[1]Neurobiology Research Unit, Copenhagen University Hospital, Rigshospitalet, Copenhagen, Denmark

[2]Department of Neurosurgery, University of Leipzig, Germany

[3]Helmholtz-Zentrum Dresden-Rossendorf, Institute of Radiopharmaceutical Cancer Research, Research Site Leipzig, Dept. of Neuroradiopharmaceuticals, Permoserstrasse 15, 04318 Leipzig, Germany

Keywords: traumatic brain injury, translocator protein 18 kDa, TSPO, microglia, neuroinflammation

* Correspondence:
Jens D. Mikkelsen, Neurobiology Research Unit, Copenhagen University Hospital, Rigshospitalet, Blegdamsvej 9, DK-2100, Copenhagen, Denmark
Tel: +45 3545 6701; Fax: +45 3545 6713 E-mail: jens.mikkelsen@nru.dk

Abstract

After traumatic brain injury (TBI), secondary injuries develop, including neuro-inflammatory processes that contribute to long-lasting impairments. These secondary injuries represent potential targets for treatment and diagnostics. The translocator protein 18 kDa (TSPO) is expressed in activated microglia cells and upregulated in response to brain injury and therefore a potential biomarker of the neuro-inflammatory processes. Second-generation radioligands of TSPO, such as [^{123}I]CLINDE, have a higher signal-to-noise ratio as the prototype ligand PK11195. [^{123}I]CLINDE has been employed in human studies using Single-photon emission computed tomography to image the neuro-inflammatory response after stroke. In this study, we used the same tracer in a rat model of TBI to determine changes in TSPO expression.

Adult Sprague-Dawley rats were subjected to moderate Controlled-Cortical-Impact injury at the M1 motor cortex, and sacrificed at 6h, 24h, 72h, and 28 days post-surgery. TSPO expression was assessed in brain sections employing [^{123}I]CLINDE *in vitro* autoradiography.

From 24 h to 28 days post-surgery, injured animals exhibited a marked and time-dependent increase of CLINDE binding in the ipsilateral motor, somatosensory and parietal cortex, as well as in the hippocampus and thalamus. Interestingly, binding was also significantly elevated in the contralateral M1 motor cortex following TBI. Craniotomy without TBI caused a less marked increase in [^{123}I]CLINDE binding, restricted to the ipsilateral hemisphere. Radioligand binding was consistent with an increase in TSPO mRNA expression and CD11b immunoreactivity at the contusion site.

This study demonstrates the applicability of [^{123}I]CLINDE for detailed regional and quantitative assessment of glial activity in experimental models of TBI.

Introduction

Traumatic brain injury (TBI) is a disease with many different symptoms and transient to life-long cognitive and sensorimotor disabilities. The complex and intertwined mechanisms responsible for these disabilities can be roughly separated in primary and secondary injuries. The primary injury is the initial biomechanical trauma (Stemper and Pintar 2014), a process that causes neuronal, axonal and vascular damage induced by the kinetic energy. However, this primary trauma triggers a cascade of secondary processes that result in excitotoxicity, necrosis, apoptosis, autophagy and free radical formation (Blennow et al. 2012). Due to this cascade of events, TBI is considered to be a chronic disease (Masel and DeWitt 2010). Furthermore this implicates that the pathological processes take place in the injured brain at different times after the injury, where some are beneficial to recovery and others are triggered by and aggravating the initial damage.

One of the key features of TBI is the robust inflammatory response, characterized by release of cytokines and chemokines (Woodcock and Morganti-Kossmann 2013), activation of glia cells in the brain and invasion of peripheral immune cells, e.g. leukocytes and macrophages due to leakiness of the blood-brain-barrier (Lozano et al. 2015). The inflammatory response in TBI represents both beneficial/restorative and detrimental/degenerative mechanisms in the restorative process (Schwarzmaier and Plesnila 2014). Pro-inflammatory stimuli trigger morphological and functional changes of microglia, the principal immune cells of the brain, termed “microglia activation”. An important result of microglia activation is the change of the translocator protein 18 kDa (TSPO), located at the contact sites between the outer and inner mitochondrial membrane (Jaremko et al. 2014). This protein is expressed at low levels in the healthy brain, but markedly upregulated in response to injury (Papadopoulos and Lecanu 2009) and neuroinflammation (Chen and Guilarte 2008). This upregulation is associated with microglia activation, however not restricted to these cells alone. TSPO upregulation was also reported on astrocytes (Kuhlmann and Guilarte 2000; Maeda et al. 2007) co-localized with selective radioligand binding (Yu et al. 2010). Irrespectively of the triggering event and underlying cellular source of the TSPO changes, its upregulation is regarded as an important

biomarker of neuroinflammation (Liu et al. 2014) and brain injury (Papadopoulos and Lecanu 2009) . Notably, imaging changes in TSPO binding with selective radiotracers in patients offers a unique opportunity to study inflammatory processes *in vivo*. For this purpose, a number of radiolabelled small molecules with superior affinity and selectivity, compared to the prototypical TSPO ligand PK11195, have been developed (Trapani et al. 2013). Specifically, 6-chloro-2-(4'-(123)I-iodophenyl)-3-(N,N-diethyl)-imidazo[1,2-a]pyridine-3-acetamide (CLINDE) is such a second-generation ligand, characterized by high affinity, brain uptake and signal to noise ratio (Arlicot et al. 2008; Mattner et al. 2008). In preclinical settings, CLINDE was found to be selective for TSPO, characterized by lack of specific binding in TSPO knock-out mice (Banati et al. 2014) and robust upregulation of TSPO binding was previously demonstrated in animal models of e.g. excitotoxicity, focal ischemia and experimental autoimmune encephalomyelitis (Mattner et al. 2005; Arlicot et al. 2008; Arlicot et al. 2010; Mattner et al. 2011; Arlicot et al. 2014). Furthermore, our research group recently applied CLINDE to image regulation of TSPO in patients with cerebral stroke or glioblastoma, where it was found to predict infarct size and tumour progression, respectively (Feng et al. 2014; Jensen et al. 2015a). More importantly, CLINDE was able to show the effect of immunotherapy in a patient suffering from anti-NMDA receptor encephalitis (Jensen et al. 2015b). However, as most of the second-generation TSPO ligands (Owen et al. 2010), CLINDE binding in humans is affected by the rs6971 single-nucleotide polymorphism, resulting in high, mixed and low-affinity binders (Feng et al. 2014). In animal models of TBI, CLINDE might serve as a biomarker to monitor and quantify therapeutic effects. In order to study the time- and region-dependent changes of TSPO after TBI, we assessed TSPO binding by employing *in vitro* [^{123}I]CLINDE autoradiography.

Materials and methods

The experimental protocols were approved by the local ethic committee. All animal experiments were authorized by the local governmental authorities (license number TVV 22/09).

Controlled Cortical Impact model of Traumatic Brain Injury

For the experiments, a total of 64 male, adult (55-70 days, weight: 291±31 g) Sprague-Dawley rats (Janvier, France) were used with post-surgery survival time-points of 6, 24, 72 hours and 28 days. Each time point consisted of 16 rats that were randomly assigned to receive either TBI (n=5), craniotomy (n=3) or sham operation (n=5). Additional three rats per group received no anaesthesia or surgery and served as naive controls.

Prior to the experiments, animals were kept in cages (4-6 in each) under controlled conditions of temperature and humidity and were subjected to a 12/12 hours dark/light-cycle. After surgery, animals were housed in individual cages with nutrition and water ad libitum.

Surgical procedures and the injury model were previously described in detail (Donat et al. 2007; Donat et al. 2008). Rats were intramuscularly anaesthesized with fentanyl (0.005 mg/kg, Janssen, Germany), midazolam (2 mg/kg, Ratiopharm, Germany) and medetomidine (0.15 mg/kg, Pfizer, Germany). The animals received perioperative analgesia with metamizole (100 mg/kg, Ratiopharm, Germany).

Body temperature was maintained at 37°C during surgery through a thermistor rectal probe feedback-controlled heating pad (FHC Inc., USA). Subsequently, the animals were placed in a stereoteactic frame, the hair was removed and the scalp disinfected with povidoneiodine. A midline incision exposed the skull (Sham, Craniotomy and TBI group).

Animals (craniotomy and TBI group) were subjected to a unilateral 6 mm circular craniotomy with an electrical dental drill over the M1 motor cortex (3.5 mm posterior, +4.0 mm lateral to bregma) of the left hemisphere, with intact dura. The bone flap was stored in sterile saline until reimplantation.

For TBI, a unilateral focal injury (TBI group, Controlled-Cortical-Impact, CCI) to the left hemisphere was induced with a 5-mm-diameter rounded metal impactor, electromagnetically driven by a CCI device (Custom Design and Fabrication, Virginia Commonwealth University, USA). The exposed dura was hit by the impactor for 100 ms at a velocity of 4 m/s and a depth of 2 mm, resulting in a moderate injury (Yu et al. 2009). For craniotomy, the brain was exposed to serve as a control for the surgery procedure. Immediately after this procedure, the bone flap was replaced and fixed with a non-toxic light-curing embedding resin (TechnoVit® 7200, Heraeus Kulzer, Germany). The incision was sutured (in case of the 6 hour group, animals were stapled) and anaesthesia antagonized with a subcutaneous injection of a mixture of naloxone (0.12 mg/kg, Ratiopharm, Germany), flumazenil (0.2 mg/kg, Roche, Germany) and atipamezole (0.75 mg/kg, Pfizer, Germany). The rats were returned to individual cages and received postoperative analgesia with metamizole, once injected postoperatively (100 mg/kg metamizole i.m) and later added to the drinking water. At designated times after CCI, rats were lightly anaesthetized with the same mixture as described above and the animals subsequently decapitated. After decapitation, the brain was quickly removed and immediately frozen in -40°C 2-methylbutane for at least 30 s and stored at -80°C C for further processing.

Tissue preparation

Coronal whole-brain sections (12 µm) were cut with a cryostat microtome (MICROM HM 560, Walldorf, Germany), mounted onto untreated glass slides [25x45 mm (3 sections); Carl Roth, Germany], briefly dried at room temperature and stored at -28°C until further processing.

In vitro autoradiography of [^{123}I]CLINDE

[^{123}I]CLINDE was supplied by MAP Medical Technologies Oy (Tikkakoski, Finland), prepared according to GMP standards for clinical use with a maximum specific activity (SA) of 8800 TBq/mmol.

Autoradiography was performed similar to previously published methods with [^{125}I]CLINDE (Mattner et al. 2011). To achieve a concentration of three nMol/L, the specific activity was lowered by adding unlabelled CLINDE (supplied by Dr. N. Arlicot) to the assay buffer.

All sections were thawed for 15 minutes at room temperature (RT) and 20 min pre-incubated in assay buffer (50 mM TRIS-HCl, pH 7.4/RT). Afterwards, the sections were incubated under gentle agitation for 60 minutes at RT with assay buffer containing the radioligand. Non-specific binding was determined on adjacent sections of the same animal with the radioligand and 10 µM PK11195 (Biotrend, Switzerland). Subsequently, slides were washed for 2x2 min in washing buffer (50 mM TRIS-HCl, pH 7.4/4°C) and 30 sec in ice-cold ultra-pure water. All slides were then air-stream dried for 20 minutes and exposed to BAS-SR2540 imaging plates (Fuji Film, Tokyo, Japan) together with ^{14}C- standards (0146N, American Radiolabelled Chemicals, USA) for 20 minutes.

Autoradiography data analysis

For analysis of [^{123}I]CLINDE binding, imaging plates were scanned using a Bioimager (BAS 2500, Fuji), converted to TIF-files using the manufacturer's software and analysed in QuantityOne (BioRad, Waltham, USA). Regions of interest (ROIs) were drawn over the primary motor cortex, hippocampus, thalamus, parietal association and barrel field of the primary somatosensory cortex, confirmed by Nissl and Gallays staining (Figure 1/2 B) on adjacent sections of naïve animals (Figure 1/2 C). All ROIs were determined in each single animal (within-subject design) in triplicate (three sections per animal). Mean values of optical density per mm^2 were converted to radioactive concentration using a linear regression derived from the ^{14}C-radioactive standards. A global background was subtracted and the values were normalized to the mean values of the corresponding brain regions of the naïve group. Final values are expressed as percentage of mean naïve.

Immunohistochemistry

Coronal sections were fixed for 20 min in 4% paraformaldehyde solution (in phosphate buffered saline, PBS) at 4°C. Slides were washed afterwards 3x10 min in PBS and were dried at RT.

Sections were quenched with hydrogen peroxide (0.6%) and MeOH (10%) in PBS. Slides were washed again (3x5 min) in 1x PBS and afterwards incubated in blocking solution (5% normal goat serum, 2% BSA, 0.2% Triton X-100 in PBS) to block endogenous peroxidase and non-specific binding, respectively. Sections were then incubated overnight at 4°C in a humidified chamber with the primary mouse monoclonal antibody OX-42 (1:500; AbD Serotec, Puchheim, Germany), recognising the complement type 3 receptor present on cells of microglial lineage, as well as granulocytes and dendritic cells (Robinson et al. 1986). Afterwards, the sections were rinsed 3x10 min in PBS and the incubated 90 min in secondary polyclonal anti-mouse biotinylated (1:1000 with 2% BSA and 0.2% TX in PBS, Jackson ImmunoResearch, West Grove, USA). Slides were washed again 3x10 min in PBS before incubation for 1 h with 0.4% avidin–biotin-peroxidase complex solution (Vectastain ABC kit, Vector Laboratories, Burlingame, USA) in PBS with 0.1% TX. After rinsing (3x10 min in PBS), the immunoreaction was developed with diaminobenzidine as chromagen (0.1% DAB and 0.03% H_2O_2 in Tris–HCl, pH 7.6). Slides were dehydrated in an ascending series of ethanol, followed by xylene and mounted in Pertex. Images were digitized with a CCD scanner (HP ScanJet 3800).

Real Time Quantitative PCR

For determination of mRNA levels of TSPO with qPCR, additional 5 animals were subjected to TBI or sham-operation.

Total RNA was extracted from sampled frozen tissue blocks (~1mm^3, taken from the injured M1 motor cortex), with an RNeasy Mini Kit (Qiagen, Hilden, Germany) according to the manufacturer's protocol, and dissolved in RNase-free water. The content of RNA was determined with a Nanodrop ND-2000 spectrophotometer (Thermo Fisher Scientific, Waltham, USA). Extracted RNA was reverse transcribed into single-stranded cDNA with the ImPromII™

Reverse Transcription System (Promega, Madison, USA) according to the manufacturer's protocol using oligo(dT) 15 primers, 6 mM $MgCl_2$, and 20 units of RNase inhibitor. Real-time RT-qPCR reactions were performed in a total volume of 20 µl, containing 5 µl sample cDNA, 10 µl 2×Brilliant II SYBR® Green qPCR Master Mix (Agilent Technologies, Santa Clara, USA), 15 pmol each of the forward and reverse primer (DNA Technology, Aarhus, Denmark), and combined with distilled water to the final volume. Non-template and non-enzyme controls were also included.

The primers used in these experiments were confirmed by gel electrophoresis with the sequence as following. GAPDH (NM_017008.4) Forward: CATCAAGAAGGTGGTGAAGCA, Reverse: CTGTTGAAGTCACAGGAGACA and TSPO (NM_012515) Forward: GCTGCCCGCTTGCTGTATCCT and Reverse CCCTCGCCGACCAGAGTTATCA according to (Lavisse et al. 2012).

PCR was performed on a Light Cycler 480 (Roche, Indianapolis, USA) with a 130 sec preincubation at 95 °C followed by 45 cycles of 5 s at 95 °C, 30 s at 60 °C and 1 cycle of 1 s at 50 °C and 5 min at 40 °C. Each primer pair was validated by using serially diluted cDNA from a randomly selected RNA sample to establish a standard curve. Quantification of mRNA expression was performed according to the comparative CT method (Schmittgen and Livak 2008). For each sample, the amount of target mRNA was normalized to that of the reference gene GAPDH.

Statistical processing

Differences between groups (autoradiography and RT-qPCR) were tested with an unpaired two-tailed Student's *t*-test, with significance levels of $\alpha=0.05$.

Insert Figure 1 about here

Results

In vitro autoradiography of [^{123}I]CLINDE

In vitro autoradiography employing the TSPO selective radioligand [^{123}I]CLINDE showed that binding in the brain of sham-operated and drug/surgery naïve animals was very low and nearly uniform at all investigated time points. Higher binding in these control groups was observed in the rhinal fissure, rhinal incisura at the motor cortex level (Figure 1A). Sham and naïve animals showed slightly higher binding in subcortical structures, especially in thalamic and hypothalamic structures, the hippocampal fissure and over the ventricular ependymal in the dorsal part and the posterior portion of the 3rd ventricle as well as in the lateral ventricles (Figure 2A).

Nonspecific binding, assessed with 10 µM PK11195, was uniform across all investigated groups, indicating high selectivity and signal-to-noise ratio of the radioligand.

Time-dependent increase of [^{123}I]CLINDE binding after focal TBI

Binding at the injury site (Interaural 12.20 mm, Bregma 3.20 mm):

In TBI-injured animals, a distinct temporal and brain regional upregulation of TSPO binding was observed in the proximity of the injury as demonstrated in representative autoradiographs in Figure 1A and 3A.

At 6 hours post injury, no significant changes of [^{123}I]CLINDE binding in the cortex were observed. However, after 24 h, TBI-injured animals exhibited a two-fold increase in radioligand binding compared to craniotomy and sham ($P<0.05$ and $P<0.01$, respectively). Craniotomy alone also caused a significantly higher binding as compared to sham ($P<0.05$) (Fig. 3A).

CLINDE binding was maximally elevated at 72 h post-surgery, in TBI animals as well as in craniotomized animals (as compared to the sham-operated group, $P < 0.01$). However, there was no significant difference in the CLINDE binding level between TBI and craniotomy at this time point.

At 28 days post-surgery, CLINDE binding remained approximately two-fold elevated in the TBI-injured and craniotomized animals, as compared to shams ($P<0.001$), but no differences were found between these two groups.

Crainotomized animals showed no changes in CLINDE binding in the contralateral motor cortex. In contrast, all animals subjected to TBI exhibited a moderately increased CLINDE binding in the contralateral motor cortex both at 24 and 72 h post-surgery (Fig. 1A and 3A, $P<0.05$).

Insert Figure 2 about here

Binding in other regions (Interaural 5.20 mm, Bregma -3.80 mm):

As illustrated in autoradiographs in Figure 2A/3B, both TBI and craniotomized controls animals exhibited a distinct and time-dependent pattern of CLINDE binding in brain regions that were not directly affected by the mechanical injury.

At 6 h post-surgery, only minor changes in hippocampus, thalamus, parietal association cortex and barrel field of the primary somatosensory cortex were observed.

The parietal and somatosensory cortices showed a moderate but significant increase of [^{123}I]CLINDE binding at 24 h post-surgery in the TBI-injured ($P<0.01$) and craniotomy ($P<0.01$) groups compared to sham, but not between each other.

The most pronounced increases in [^{123}I]CLINDE binding were found at 72 hours post-surgery. In the parietal cortex, TBI caused a nearly three-fold increase of radioligand binding ($P<0.001$), similar to the two-fold increase of craniotomized animals ($P<0.001$) compared to the sham group. This pattern was also observed in the somatosensory cortex in TBI-injured (+239%, $P<0.001$) and craniotomized animals (+155%, $P<0.01$). Additionally, the whole hippocampus of rats subjected to TBI showed a small but significantly elevated binding (+36%, $P<0.01$).

In contrast, no significant hippocampal alterations were found in the subacute phase at 28 days post-surgery. Both parietal (+77%, $P<0.001$) and somatosensory (+87%, $P<0.001$) cortices showed elevated CLINDE binding in animal subjected to TBI and craniotomy (+77%, $P<0.05$; +80%, $P<0.01$) after 28 days.

In the thalamus (primarily the ventral posteromedial thalamic nucleus), changes were only detected at 28 d post-surgery, and not at any other time-point. The increase in radioligand

binding was significantly different from sham-operated ($P<0.01$) and craniotomized rats ($P<0.05$). Across all time points, no significant differences were observed in the corresponding structures of the contralateral hemisphere (data not shown).

Insert Figure 3 about here.

TSPO mRNA levels correspond to increases of [^{123}I]CLINDE binding in the motor cortex at 72 hours post injury.

In extracts from the M1 motor cortex of animals subjected to TBI, an eight-fold increase of TSPO mRNA was found at 72 hours post injury when compared to sham ($P<0.0001$) (Fig 4).

Insert Figure 4 about here.

OX-42 immunopositive cells are concentrated in the contusion of the injured M1 motor cortex and match the distribution of [^{123}I]CLINDE binding at 72 hours post injury.

Immunostaining using the OX-42 (CD11b) antibody revealed a high number of OX-42 immunopositive cells in the contusion (Figure 5 left image) at 72 h post-surgery. The distribution of OX-42 immunoreactivity overlapped with the strongest increase in radioligand binding (Figure 5 middle and right image).

Insert Figure 5 about here.

Discussion

This study investigated changes in TSPO expression after TBI, employing the selective radioligand [^{123}I]CLINDE. CLINDE is a second-generation TSPO ligand, with a high signal-to-noise ratio, low nanomolar affinity (Mattner et al. 2008) and absence of specific binding in TSPO knockout mice (Banati et al. 2014). The observed brain regional TSPO binding pattern was similar to that reported for other TSPO radioligands (Banati et al. 1997).

CLINDE is of clinical relevance, as it has been used recently to image changes of TSPO in patients with cerebral stroke and glioblastoma, respectively (Feng et al. 2014; Jensen et al. 2015a; Jensen et al. 2015b). The low expression of TSPO in the healthy brain of man, rodents and nonhuman primates (Collste et al. 2015; Lavisse et al. 2015; Toth et al. 2015) and the robust upregulation in response to brain injury (Liu et al. 2014), allows a qualitative and quantitative assessment of neuroinflammation-associated changes. This study further supports the use of [^{123}I]CLINDE for detecting changes in TSPO binding after brain injury.

Glia cells are activated after TBI, leading to reactive astrocytic gliosis (Burda and Sofroniew 2014) and microglia activation (Norden et al. 2015) and both processes are implicated in the long-term neuropathology of the disease (reviewed in (Faden et al. 2015). Modulation of the neuro-inflammatory response after TBI is therefore regarded as an important treatment strategy. Because microglia exert both neuroprotective and neurotoxic functions, depending on their activation pattern and phenotype (Benarroch 2013), it must be emphasized that changes in TSPO binding represents a composite measure of both effects.

In the present study, a strong increase in [^{123}I]CLINDE binding was found 24 hours post-TBI at the site of the injury, peaking at 72 hours and was still significantly elevated in the subacute phase after 28 days. This temporal profile is similar to that reported in other TBI models (Raghavendra Rao et al. 2000; Yu et al. 2010; Cao et al. 2012). In addition, there is a remarkable match of *in vitro* binding and *in vivo* uptake of [^{18}F]DPA-714 after transient focal ischemia, especially one month post-injury (Martin et al. 2010), which lends support to the translatability of *in vitro* CLINDE binding assay to *in vivo* imaging.

qPCR analysis revealed an increase of TSPO mRNA in a comparable magnitude, which further demonstrates target selectivity of CLINDE and, importantly, also indicates that [^{123}I]CLINDE binding directly reflects corresponding changes in TSPO expression. qPCR allows a sensitive evaluation in very small quantity samples. Selective analysis of activated immune cells, e.g. by CD11b separation, could furthermore be used to determine microglia phenotype dynamics (Kumar et al. 2015). Depending to their phenotype, microglia can act as mediators of progressive tissue regeneration or chronic degeneration, and modulation of these processes provide potential treatment options. In contrast, molecular imaging investigates changes of the targeted protein and offers translatability to the clinics e.g. through non-invasive PET/SEPCT imaging of human subjects.

Craniotomy induced a less pronounced increase in CLINDE binding in most of the ipsilateral brain structures, likely caused by perturbations to the dura mater and the surface of the cerebral cortex and therefore subsequently induces inflammatory changes. In agreement with our observation, others have reported that craniotomy induces brain injury, behavioural impairments and a profound inflammatory response (Cole et al. 2011; Lagraoui et al. 2012). It may thus be argued that craniotomy is not an appropriate control in open-skull models of TBI, as it may potentially mask specific effects of TBI *per se* and lead to an underestimation of therapeutic effects. Our findings clearly indicate that TBI promotes a more marked brain damage and consequently larger increase in CLINDE binding. Furthermore, in contrast to TBI, craniotomy had no effect on CLINDE binding in the ipsilateral thalamus 28 days post-injury, hippocampus and in the contralateral cortex.

The delayed thalamic TSPO increase at 28 days post-TBI points to a specific vulnerability (reviewed in (Grossman and Inglese 2016), suggesting the thalamus as a target of secondary inflammation. This is frequently observed after TBI in animal models (Raghavendra Rao et al. 2000; Grossman et al. 2003; Kelso et al. 2009; Yu et al. 2010; Folkersma et al. 2011b; Cao et al. 2012) and patients (Folkersma et al. 2011a; Ramlackhansingh et al. 2011), where it correlates with persistent white matter damage (Scott et al. 2015). Similar changes are reported after stroke in rats (Myers et al. 1991) and humans (Pappata et al. 2000). This

increase in regions distal from the cortical primary injury occurs long after the initial damage and in areas known to project directly to the site of damage, i.e. the ventrolateral thalamic nuclei and in contralateral brain areas indicating that microglial activation could spread along damaged white matter tracts.

Similarly, contralateral cortical increases of TSPO radiotracer uptake were reported before (Yu et al. 2010). The underlying mechanisms for the TSPO increase in these regions are not clear, but it is tempting to speculate that activated microglia are also involved in compensatory restoration of neuronal function, which may occur at the contralateral hemisphere. In rodent models of stroke, microglia suppression leads to long-term decreases of neuronal plasticity markers, e.g. brain-derived neurotrophic factor (Madinier et al. 2009) and contralesional pyramidal tract plasticity was found to promote recovery (Liu et al. 2011; Herz et al. 2012). The detection of small, however relevant changes in TSPO binding levels in areas presumed to be associated with neuroregeneration and synaptic plasticity, requires highly sensitive TSPO tracer ligands, and our study therefore suggests that [^{123}I]CLINDE may be useful not only to detect detrimental consequences of CNS injury, but also to reveal possible regeneration potential long after the insult has taken place.

Our findings are in line with previous TBI studies where CCI injury in rats caused increased TSPO radioligand binding and mRNA levels at the contusion site (Raghavendra Rao et al. 2000; Venneti et al. 2007; Guseva et al. 2008; Kelso et al. 2009). After fluid percussion, [^{3}H]PK11195 binding was increased at day seven post injury in the somatosensory cortex and thalamus, while after 28 days only the thalamus retained the significant increase (Cao et al. 2012). Similar increases of TSPO are reported in other models of TBI (Miyazawa et al. 1995; Grossman et al. 2003; Soustiel et al. 2008).

In vivo [^{11}C]PK11195 and [^{18}F]DPA-714 uptake was increased after CCI in rats (Folkersma et al. 2011b) peaking at day 6 and slowly decreasing until 28 days post injury (Wang et al. 2014). Lateral fluid percussion injury increased uptake of [^{18}F]FE-DAA1106 in the ipsi- and contralateral cortex, striatum and thalamus (Yu et al. 2010), followed by a delayed increase in tracer accumulation in the white matter at 9 weeks post injury, indicating axonal injury.

Disruption of the blood-brain-barrier, with an immediate opening in the first hours and a delayed perturbation around three days (Baldwin et al. 1996; Baskaya et al. 1997) should be considered for *in vivo* studies. This could affect the radioligand uptake, as observed after ischemia with increased tracer delivery ratios from day four on, indicating a higher uptake in the injured hemisphere (Martin et al. 2010).

The most interesting perspective is to what extend these tracers are useful in human patients of TBI and other pathological conditions triggering neuroinflammation. Increased [^{11}C]PK11195 binding potential was found in the thalamus of patients in different studies (Folkersma et al. 2011a; Ramlackhansingh et al. 2011; Scott et al. 2015). PET imaging with [^{11}C]DPA-713 revealed overall higher distribution volumes in the thalamus and brainstem of retired football players, years after multiple concussions (Coughlin et al. 2015), demonstrating the applicability of TSPO tracers to investigate long-term inflammatory changes.

Dissecting the cellular origin of the TSPO upregulation proves difficult. Initially, resident microglia are activated in response to damage-associated molecular patterns, accompanied by *de novo* synthesis of TSPO and therefore accounting for the majority of TSPO upregulation. However, other cells also express TSPO, e.g. ED-1/CD68 positive macrophages (Lemstra et al. 2007), as previously found in our model (Härtig et al. 2013), reactive astrocytes (Raghavendra Rao et al. 2000; Venneti et al. 2007; Yu et al. 2010) and invading peripheral macrophages. In the present study, OX-42 staining was concentrated at the contusion site, showing phagocytic microglia/macrophages in the necrotic core, overlapping with the most pronounced radioligand binding, similar to previous reports (Yu et al. 2010). Because BBB opening after CCI is most pronounced in the first hours after injury, we believe that microglia and macrophages provide the largest fraction of TSPO upregulation, as shown by [^{123}I]CLINDE binding during day one and three post-injury.

In conclusion, our data shows that TSPO binding is markedly increased in response to TBI in the contusion and brain regions not directly affected by mechanical injury. An upregulation is found in the contralesional cortex and at 28 d in the ipsilateral thalamus. By employing two different control groups at all investigated time points, we demonstrate that craniotomy also

increases [^{123}I]CLINDE binding in ipsilateral brain regions, which should be taken into account when employing open-head models of TBI. [^{123}I]CLINDE might therefore be a promising radioligand to visualize and quantify the neuroprotective and/or anti-inflammatory effects of treatments in preclinical models of TBI.

Acknowledgments:

We thank Tina Spalholz and the staff of MEZ Leipzig for excellent technical support and assistance in animal experiments and Felix Fischer for assistance in tissue sectioning. CLINDE was kindly supplied by Dr. Nicolas Arlicot, Université François Rabelais de Tours, France.

This work was supported by Desirée and Niels Ydes Foundation, the Lundbeck Foundation, and the Danish Strategic Research Council (project COGNITO). The research leading to these results was supported by the European Union's Seventh Framework Programme (FP7/2007-2013) under grant agreement HEALTH-F2-2011-278850 (INMiND).

Conflict of interest

The authors declare no conflicts of interest.

References

Arlicot, N., Katsifis, A., Garreau, L., Mattner, F., Vergote, J., Duval, S., et al. (2008). Evaluation of CLINDE as potent translocator protein (18 kDa) SPECT radiotracer reflecting the degree of neuroinflammation in a rat model of microglial activation. *Eur J Nucl Med Mol Imaging, 35*(12), 2203-2211

Arlicot, N., Petit, E., Katsifis, A., Toutain, J., Divoux, D., Bodard, S., et al. (2010). Detection and quantification of remote microglial activation in rodent models of focal ischaemia using the TSPO radioligand CLINDE. *Eur J Nucl Med Mol Imaging, 37*(12), 2371-2380

Arlicot, N., Tronel, C., Bodard, S., Garreau, L., de la Crompe, B., Vandevelde, I., et al. (2014). Translocator protein (18 kDa) mapping with [^{125}I]-CLINDE in the quinolinic acid rat model of excitotoxicity: a longitudinal comparison with microglial activation, astrogliosis, and neuronal death. *Mol Imaging, 13*(2), 4-11

Baldwin, S. A., Fugaccia, I., Brown, D. R., Brown, L. V., & Scheff, S. W. (1996). Blood-brain barrier breach following cortical contusion in the rat. *J Neurosurg, 85*(3), 476-481

Banati, R. B., Middleton, R. J., Chan, R., Hatty, C. R., Kam, W. W., Quin, C., et al. (2014). Positron emission tomography and functional characterization of a complete PBR/TSPO knockout. *Nat Commun, 5*, 5452

Banati, R. B., Myers, R., & Kreutzberg, G. W. (1997). PK ('peripheral benzodiazepine')--binding sites in the CNS indicate early and discrete brain lesions: microautoradiographic detection of [^{3}H]PK11195 binding to activated microglia. *J Neurocytol, 26*(2), 77-82

Baskaya, M. K., Rao, A. M., Dogan, A., Donaldson, D., & Dempsey, R. J. (1997). The biphasic opening of the blood-brain barrier in the cortex and hippocampus after traumatic brain injury in rats. *Neurosci Lett, 226*(1), 33-36

Benarroch, E. E. (2013). Microglia: Multiple roles in surveillance, circuit shaping, and response to injury. *Neurology, 81*(12), 1079-1088

Blennow, K., Hardy, J., & Zetterberg, H. (2012). The neuropathology and neurobiology of traumatic brain injury. *Neuron, 76*(5), 886-899

Burda, J. E., & Sofroniew, M. V. (2014). Reactive gliosis and the multicellular response to CNS damage and disease. *Neuron, 81*(2), 229-248

Cao, T., Thomas, T. C., Ziebell, J. M., Pauly, J. R., & Lifshitz, J. (2012). Morphological and genetic activation of microglia after diffuse traumatic brain injury in the rat. *Neuroscience, 225*, 65-75

Chen, M. K., & Guilarte, T. R. (2008). Translocator protein 18 kDa (TSPO): molecular sensor of brain injury and repair. *Pharmacol Ther, 118*(1), 1-17

Cole, J. T., Yarnell, A., Kean, W. S., Gold, E., Lewis, B., Ren, M., et al. (2011). Craniotomy: true sham for traumatic brain injury, or a sham of a sham? *J Neurotrauma, 28*(3), 359-369

Collste, K., Forsberg, A., Varrone, A., Amini, N., Aeinehband, S., Yakushev, I., et al. (2015). Test-retest reproducibility of [^{11}C]PBR28 binding to TSPO in healthy control subjects. *Eur J Nucl Med Mol Imaging*

Coughlin, J. M., Wang, Y., Munro, C. A., Ma, S., Yue, C., Chen, S., et al. (2015). Neuroinflammation and brain atrophy in former NFL players: An in vivo multimodal imaging pilot study. *Neurobiol Dis, 74*, 58-65

Donat, C. K., Schuhmann, M. U., Voigt, C., Nieber, K., Schliebs, R., & Brust, P. (2007). Alterations of acetylcholinesterase activity after traumatic brain injury in rats. *Brain Inj, 21*(10), 1031-1037

Donat, Cornelius K., Schuhmann, Martin U., Voigt, Cornelia, Nieber, Karen, Deuther-Conrad, Winnie, & Brust, Peter (2008). Time-dependent alterations of cholinergic markers after experimental traumatic brain injury. *Brain Res, 1246*, 167-177

Faden, A. I., Wu, J., Stoica, B. A., & Loane, D. J. (2015). Progressive inflammatory-mediated neurodegeneration after traumatic brain or spinal cord injury. *Br J Pharmacol*

Feng, L., Svarer, C., Thomsen, G., de Nijs, R., Larsen, V. A., Jensen, P., et al. (2014). In vivo quantification of cerebral translocator protein binding in humans using 6-chloro-2-(4'-^{123}I-iodophenyl)-3-(N,N-diethyl)-imidazo[1,2-a]pyridine-3-acetamid e SPECT. *J Nucl Med, 55*(12), 1966-1972

Folkersma, H., Boellaard, R., Yaqub, M., Kloet, R. W., Windhorst, A. D., Lammertsma, A. A., et al. (2011a). Widespread and prolonged increase in (R)-^{11}C-PK11195 binding after traumatic brain injury. *J Nucl Med, 52*(8), 1235-1239

Folkersma, H., Foster Dingley, J. C., van Berckel, B. N., Rozemuller, A., Boellaard, R., Huisman, M. C., et al. (2011b). Increased cerebral (R)-[^{11}C]-PK11195 uptake and glutamate release in a rat model of traumatic brain injury: a longitudinal pilot study. *J Neuroinflammation, 8*, 67

Grossman, E. J., & Inglese, M. (2016). The Role of Thalamic Damage in Mild Traumatic Brain Injury. *J Neurotrauma, 33*(2), 163-167

Grossman, R., Shohami, E., Alexandrovich, A., Yatsiv, I., Kloog, Y., & Biegon, A. (2003). Increase in peripheral benzodiazepine receptors and loss of glutamate NMDA receptors in a mouse model of closed head injury: a quantitative autoradiographic study. *Neuroimage, 20*(4), 1971-1981

Guseva, M. V., Hopkins, D. M., Scheff, S. W., & Pauly, J. R. (2008). Dietary choline supplementation improves behavioral, histological, and neurochemical outcomes in a rat model of traumatic brain injury. *J Neurotrauma, 25*(8), 975-983

Härtig, W., Michalski, D., Seeger, G., Voigt, C., Donat, C. K., Dulin, J., et al. (2013). Impact of 5-lipoxygenase inhibitors on the spatiotemporal distribution of inflammatory cells and neuronal COX-2 expression following experimental traumatic brain injury in rats. *Brain Res, 1498*, 69-84

Herz, J., Reitmeir, R., Hagen, S. I., Reinboth, B. S., Guo, Z., Zechariah, A., et al. (2012). Intracerebroventricularly delivered VEGF promotes contralesional corticorubral plasticity after focal cerebral ischemia via mechanisms involving anti-inflammatory actions. *Neurobiol Dis, 45*(3), 1077-1085

Jaremko, L., Jaremko, M., Giller, K., Becker, S., & Zweckstetter, M. (2014). Structure of the mitochondrial translocator protein in complex with a diagnostic ligand. *Science, 343*(6177), 1363-1366

Jensen, P., Feng, L., Law, I., Svarer, C., Knudsen, G. M., Mikkelsen, J. D., et al. (2015a). TSPO Imaging in Glioblastoma Multiforme: A Direct Comparison Between ^{123}I-CLINDE SPECT, ^{18}F-FET PET, and Gadolinium-Enhanced MR Imaging. *J Nucl Med, 56*(9), 1386-1390

Jensen, P., Kondziella, D., Thomsen, G., Dyssegaard, A., Svarer, C., & Pinborg, L. H. (2015b). Anti-NMDAR encephalitis: demonstration of neuroinflammation and the effect of immunotherapy. *Neurology, 84*(8), 859

Kelso, M. L., Scheff, S. W., Pauly, J. R., & Loftin, C. D. (2009). Effects of genetic deficiency of cyclooxygenase-1 or cyclooxygenase-2 on functional and histological outcomes following traumatic brain injury in mice. *BMC Neurosci, 10*, 108

Kuhlmann, A. C., & Guilarte, T. R. (2000). Cellular and subcellular localization of peripheral benzodiazepine receptors after trimethyltin neurotoxicity. *J Neurochem, 74*(4), 1694-1704

Kumar, A., Alvarez-Croda, D. M., Stoica, B. A., Faden, A. I., & Loane, D. J. (2015). Microglial/Macrophage Polarization Dynamics following Traumatic Brain Injury. *J Neurotrauma*

Lagraoui, M., Latoche, J. R., Cartwright, N. G., Sukumar, G., Dalgard, C. L., & Schaefer, B. C. (2012). Controlled cortical impact and craniotomy induce strikingly similar profiles of inflammatory gene expression, but with distinct kinetics. *Front Neurol, 3*, 155

Lavisse, S., Guillermier, M., Herard, A. S., Petit, F., Delahaye, M., Van Camp, N., et al. (2012). Reactive astrocytes overexpress TSPO and are detected by TSPO positron emission tomography imaging. *J Neurosci, 32*(32), 10809-10818

Lavisse, S., Inoue, K., Jan, C., Peyronneau, M. A., Petit, F., Goutal, S., et al. (2015). [^{18}F]DPA-714 PET imaging of translocator protein TSPO (18 kDa) in the normal and excitotoxically-lesioned nonhuman primate brain. *Eur J Nucl Med Mol Imaging, 42*(3), 478-494

Lemstra, A. W., Groen in't Woud, J. C., Hoozemans, J. J., van Haastert, E. S., Rozemuller, A. J., Eikelenboom, P., et al. (2007). Microglia activation in sepsis: a case-control study. *J Neuroinflammation, 4*, 4

Liu, G. J., Middleton, R. J., Hatty, C. R., Kam, W. W., Chan, R., Pham, T., et al. (2014). The 18 kDa translocator protein, microglia and neuroinflammation. *Brain Pathol, 24*(6), 631-653

Liu, Z., Li, Y., Zhang, R. L., Cui, Y., & Chopp, M. (2011). Bone marrow stromal cells promote skilled motor recovery and enhance contralesional axonal connections after ischemic stroke in adult mice. *Stroke, 42*(3), 740-744

Lozano, D., Gonzales-Portillo, G. S., Acosta, S., de la Pena, I., Tajiri, N., Kaneko, Y., et al. (2015). Neuroinflammatory responses to traumatic brain injury: etiology, clinical consequences, and therapeutic opportunities. *Neuropsychiatr Dis Treat, 11*, 97-106

Madinier, A., Bertrand, N., Mossiat, C., Prigent-Tessier, A., Beley, A., Marie, C., et al. (2009). Microglial involvement in neuroplastic changes following focal brain ischemia in rats. *PLoS One, 4*(12), e8101

Maeda, J., Higuchi, M., Inaji, M., Ji, B., Haneda, E., Okauchi, T., et al. (2007). Phase-dependent roles of reactive microglia and astrocytes in nervous system injury as delineated by imaging of peripheral benzodiazepine receptor. *Brain Res, 1157*, 100-111

Martin, A., Boisgard, R., Theze, B., Van Camp, N., Kuhnast, B., Damont, A., et al. (2010). Evaluation of the PBR/TSPO radioligand [(18)F]DPA-714 in a rat model of focal cerebral ischemia. *J Cereb Blood Flow Metab, 30*(1), 230-241

Masel, B. E., & DeWitt, D. S. (2010). Traumatic brain injury: a disease process, not an event. *J Neurotrauma, 27*(8), 1529-1540

Mattner, F., Bandin, D. L., Staykova, M., Berghofer, P., Gregoire, M. C., Ballantyne, P., et al. (2011). Evaluation of [^{123}I]-CLINDE as a potent SPECT radiotracer to assess the degree of astroglia

activation in cuprizone-induced neuroinflammation. *Eur J Nucl Med Mol Imaging, 38*(8), 1516-1528

Mattner, F., Katsifis, A., Staykova, M., Ballantyne, P., & Willenborg, D. O. (2005). Evaluation of a radiolabelled peripheral benzodiazepine receptor ligand in the central nervous system inflammation of experimental autoimmune encephalomyelitis: a possible probe for imaging multiple sclerosis. *Eur J Nucl Med Mol Imaging, 32*(5), 557-563

Mattner, F., Mardon, K., & Katsifis, A. (2008). Pharmacological evaluation of [^{123}I]-CLINDE: a radioiodinated imidazopyridine-3-acetamide for the study of peripheral benzodiazepine binding sites (PBBS). *Eur J Nucl Med Mol Imaging, 35*(4), 779-789

Miyazawa, N., Diksic, M., & Yamamoto, Y. (1995). Chronological study of peripheral benzodiazepine binding sites in the rat brain stab wounds using [^{3}H] PK-11195 as a marker for gliosis. *Acta Neurochir (Wien), 137*(3-4), 207-216

Myers, R., Manjil, L. G., Frackowiak, R. S., & Cremer, J. E. (1991). [^{3}H]PK 11195 and the localisation of secondary thalamic lesions following focal ischaemia in rat motor cortex. *Neurosci Lett, 133*(1), 20-24

Norden, D. M., Muccigrosso, M. M., & Godbout, J. P. (2015). Microglial priming and enhanced reactivity to secondary insult in aging, and traumatic CNS injury, and neurodegenerative disease. *Neuropharmacology, 96*(Pt A), 29-41

Owen, D. R., Howell, O. W., Tang, S. P., Wells, L. A., Bennacef, I., Bergstrom, M., et al. (2010). Two binding sites for [3H]PBR28 in human brain: implications for TSPO PET imaging of neuroinflammation. *J Cereb Blood Flow Metab, 30*(9), 1608-1618

Papadopoulos, V., & Lecanu, L. (2009). Translocator protein (18 kDa) TSPO: an emerging therapeutic target in neurotrauma. *Exp Neurol, 219*(1), 53-57

Pappata, S., Levasseur, M., Gunn, R. N., Myers, R., Crouzel, C., Syrota, A., et al. (2000). Thalamic microglial activation in ischemic stroke detected in vivo by PET and [^{11}C]PK1195. *Neurology, 55*(7), 1052-1054

Paxinos, G., & Watson, C. (1998). *The Rat Brain in Stereotaxic Coordinates* (4th edition ed.). San Diego: Academic Press.

Raghavendra Rao, V. L., Dogan, A., Bowen, K. K., & Dempsey, R. J. (2000). Traumatic brain injury leads to increased expression of peripheral-type benzodiazepine receptors, neuronal death, and activation of astrocytes and microglia in rat thalamus. *Exp Neurol, 161*(1), 102-114

Ramlackhansingh, A. F., Brooks, D. J., Greenwood, R. J., Bose, S. K., Turkheimer, F. E., Kinnunen, K. M., et al. (2011). Inflammation after trauma: microglial activation and traumatic brain injury. *Ann Neurol, 70*(3), 374-383

Robinson, A. P., White, T. M., & Mason, D. W. (1986). Macrophage heterogeneity in the rat as delineated by two monoclonal antibodies MRC OX-41 and MRC OX-42, the latter recognizing complement receptor type 3. *Immunology, 57*(2), 239-247

Schmittgen, T. D., & Livak, K. J. (2008). Analyzing real-time PCR data by the comparative C(T) method. *Nat Protoc, 3*(6), 1101-1108

Schwarzmaier, S. M., & Plesnila, N. (2014). Contributions of the immune system to the pathophysiology of traumatic brain injury - evidence by intravital microscopy. *Front Cell Neurosci, 8*, 358

Scott, G., Hellyer, P. J., Ramlackhansingh, A. F., Brooks, D. J., Matthews, P. M., & Sharp, D. J. (2015). Thalamic inflammation after brain trauma is associated with thalamo-cortical white matter damage. *J Neuroinflammation, 12*(1), 224

Soustiel, J. F., Palzur, E., Vlodavsky, E., Veenman, L., & Gavish, M. (2008). The effect of oxygenation level on cerebral post-traumatic apoptotsis is modulated by the 18-kDa translocator protein (also known as peripheral-type benzodiazepine receptor) in a rat model of cortical contusion. *Neuropathol Appl Neurobiol, 34*(4), 412-423

Stemper, B. D., & Pintar, F. A. (2014). Biomechanics of concussion. *Prog Neurol Surg, 28*, 14-27

Toth, M., Doorduin, J., Haggkvist, J., Varrone, A., Amini, N., Halldin, C., et al. (2015). Positron Emission Tomography studies with [^{11}C]PBR28 in the Healthy Rodent Brain: Validating SUV as an Outcome Measure of Neuroinflammation. *PLoS One, 10*(5), e0125917

Trapani, A., Palazzo, C., de Candia, M., Lasorsa, F. M., & Trapani, G. (2013). Targeting of the translocator protein 18 kDa (TSPO): a valuable approach for nuclear and optical imaging of activated microglia. *Bioconjug Chem, 24*(9), 1415-1428

Venneti, S., Wagner, A. K., Wang, G., Slagel, S. L., Chen, X., Lopresti, B. J., et al. (2007). The high affinity peripheral benzodiazepine receptor ligand DAA1106 binds specifically to microglia in a rat model of traumatic brain injury: implications for PET imaging. *Exp Neurol, 207*(1), 118-127

Wang, Y., Yue, X., Kiesewetter, D. O., Niu, G., Teng, G., & Chen, X. (2014). PET imaging of neuroinflammation in a rat traumatic brain injury model with radiolabeled TSPO ligand DPA-714. *Eur J Nucl Med Mol Imaging, 41*(7), 1440-1449

Woodcock, T., & Morganti-Kossmann, M. C. (2013). The role of markers of inflammation in traumatic brain injury. *Front Neurol, 4*, 18

Yu, I., Inaji, M., Maeda, J., Okauchi, T., Nariai, T., Ohno, K., et al. (2010). Glial cell-mediated deterioration and repair of the nervous system after traumatic brain injury in a rat model as assessed by positron emission tomography. *J Neurotrauma, 27*(8), 1463-1475

Yu, S., Kaneko, Y., Bae, E., Stahl, C. E., Wang, Y., van Loveren, H., et al. (2009). Severity of controlled cortical impact traumatic brain injury in rats and mice dictates degree of behavioral deficits. *Brain Res, 1287*, 157-163

Legend for Figures

Fig 1: Focal Traumatic Brain Injury (TBI) increases *in vitro* binding of the translocator protein 18 kDa selective radioligand [^{123}I]CLINDE in the proximity of the contusion
A: Representative autoradiographs of the rat brain after sham operation (n=5), Controlled-Cortical-Impact induced TBI (n=5) and craniotomy (n=3) at 6, 24, 72 hours and 28 days post injury including nonspecific binding from a random animal. Slice coordinates are: Interaural 12.20 mm, Bregma 3.20 mm. Red/yellow areas represent high, blue/black areas represent low binding of [^{123}I]CLINDE
B) Superimposed histological stainings (Cresyl violet and Gallays stain) of adjacent sections from drug and surgery naïve rats
C) Image showing anatomical atlas reference (Paxinos and Watson 1998) with investigated brain region (1: M1 motor cortex)

Fig 2: Focal Traumatic Brain Injury (TBI) increases *in vitro* binding of the translocator protein 18 kDa selective radioligand [^{123}I]CLINDE in remote brain regions
A: Representative autoradiographs of the rat brain after sham operation (n=5), Controlled-Cortical-Impact induced traumatic brain injury (n=5) and craniotomy (n=3) at 6, 24, 72 hours and 28 days post injury including nonspecific binding from a random animal. Slice coordinates are: Interaural 5.20 mm, Bregma -3.80 mm. Red/yellow areas represent high, blue/black areas represent low binding of [^{123}I]CLINDE.
B) Superimposed histological stainings (Cresyl violet and Gallays stain) of adjacent sections from drug and surgery naïve rats
C) Image showing anatomical atlas reference (Paxinos and Watson 1998) with investigated brain regions (1: parietal association cortex; 2: primary somatosensory cortex, barrel field; 3: hippocampus; 4: thalamus with posterior thalamic nuclear group, ventral posteromedial thalamic nucleus, centrolateral thalamic nucleus and oval paracentral thalamic nucleus)

Fig 3: Focal Traumatic Brain Injury increases binding of the translocator protein 18 kDa selective radioligand [^{123}I]CLINDE *in vitro*
A: % binding of naïve animals in sham operation (n=5), Controlled-Cortical-Impact induced traumatic brain injury (n=5) and craniotomy (n=3) at 6, 24, 72 hours and 28 days post injury. A strong increase in radioligand binding is observed in the ipsilateral M1 motor cortex in TBI/Craniotomy animals compared to sham at 24, 72 hours and 28 days post injury [^{123}I]CLINDE binding is additionally increased in the contralateral cortex after TBI at 24 and 72 hours post injury.

Data are mean ± SD. Significance tested with the Student's t-test. * P < 0.05; ** P < 0.01; ** P < 0.001

B: % binding of naïve animals in sham operation (n=5), Controlled-Cortical-Impact induced traumatic injury (n=5) and craniotomy (n=3) at 6, 24, 72 hours and 28 days post injury

A strong increase in radioligand binding is observed in the cortical areas (parietal association and primary somatosensory cortex, barrel field) in TBI/Craniotomy animals compared to sham at 24, 72 hours and 28 days post injury. Hippocampus binding is elevated at 72 hours post injury and thalamic structures show a delayed increase in binding at 28 days post injury. No differences are found in the contralateral hemisphere (data not shown)

Data are mean ± SD. Significance tested with the Student's t-test. * P < 0.05; ** P < 0.01; *** P < 0.001

Fig 4: Focal Traumatic Brain Injury increases mRNA levels of the translocator protein 18 kDa in the contusion

Increased TSPO mRNA levels in M1 motor cortex extracts of animals subjected to Controlled-Cortical-Impact induced traumatic brain injury compared to sham-operated animals as detected by RT-qPCR. *** $p < 0.0001$

Data are mean ± SD. Significance tested with the Student's t-test

Fig 5: Focal Traumatic Brain Injury increases OX-42/CD11b immunopositive cells in the vicinity of the contusion

Immunohistochemical staining for OX-42/CD11b as marker of activated microglia/macrophages

Representative photomicrographs from one animal subjected to TBI at 72 hours post injury

Photomicrograph of the injured hemisphere (left) showing immunopositive cells around the contusion and the corresponding autoradiograph of [^{123}I]CLINDE in adjacent sections (middle) Processed manual overlay of both images (right) shows that most of [^{123}I]CLINDE binding can be attributed to OX-42/CD11b immunopositive cells. Scale bar corresponds to 1 mm.

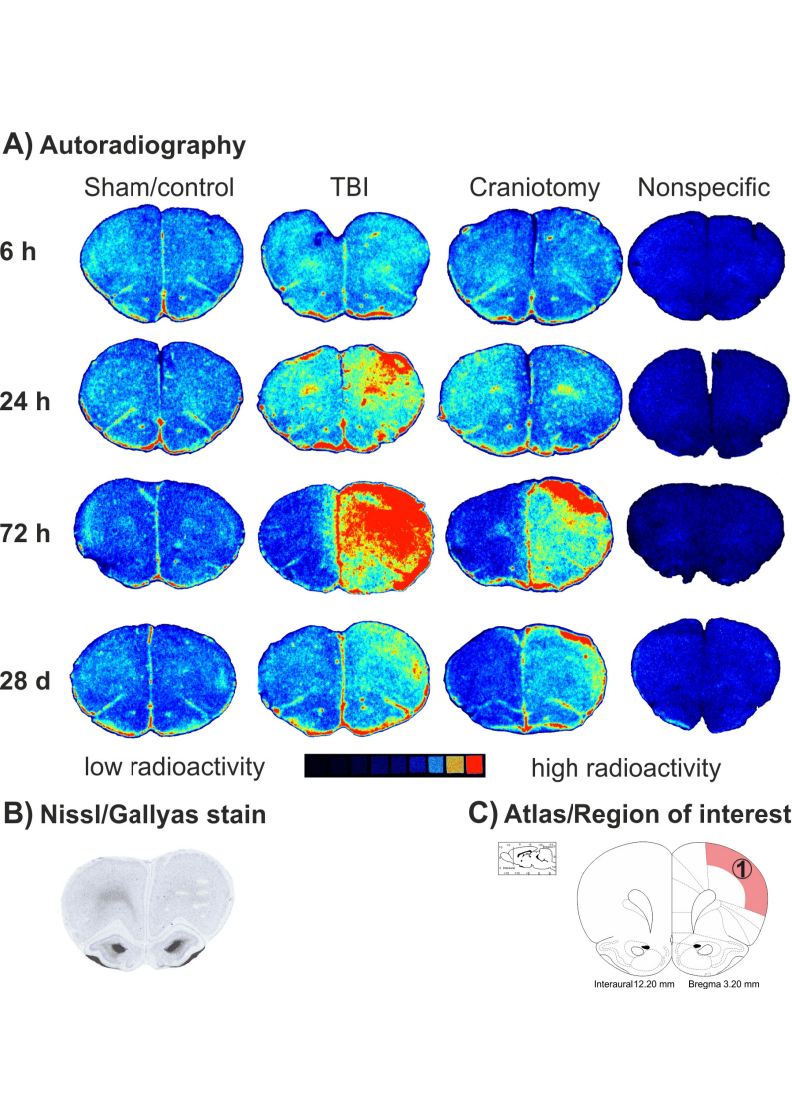
A) Autoradiography
Sham/control
TBI
Craniotomy
Nonspecific
6 h
24 h
72 h
28 d
low radioactivity
high radioactivity
B) Nissl/Gallyas stain
C) Atlas/Region of interest
1
Interaural12.20 mm
Bregma 3.20 mm

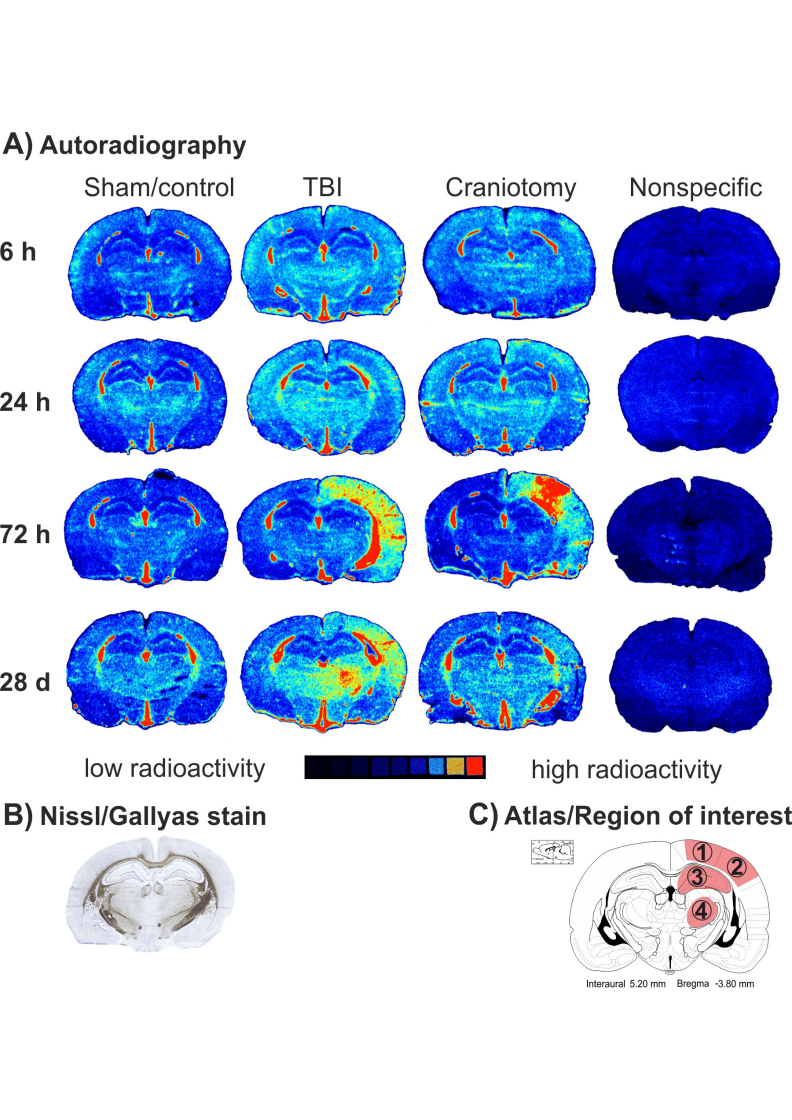
A) Autoradiography
Sham/control
TBI
Craniotomy
Nonspecific
6 h
24 h
72 h
28 d
low radioactivity
high radioactivity
B) Nissl/Gallyas stain
C) Atlas/Region of interest
1
2
3
4
Interaural 5.20 mm
Bregma -3.80 mm

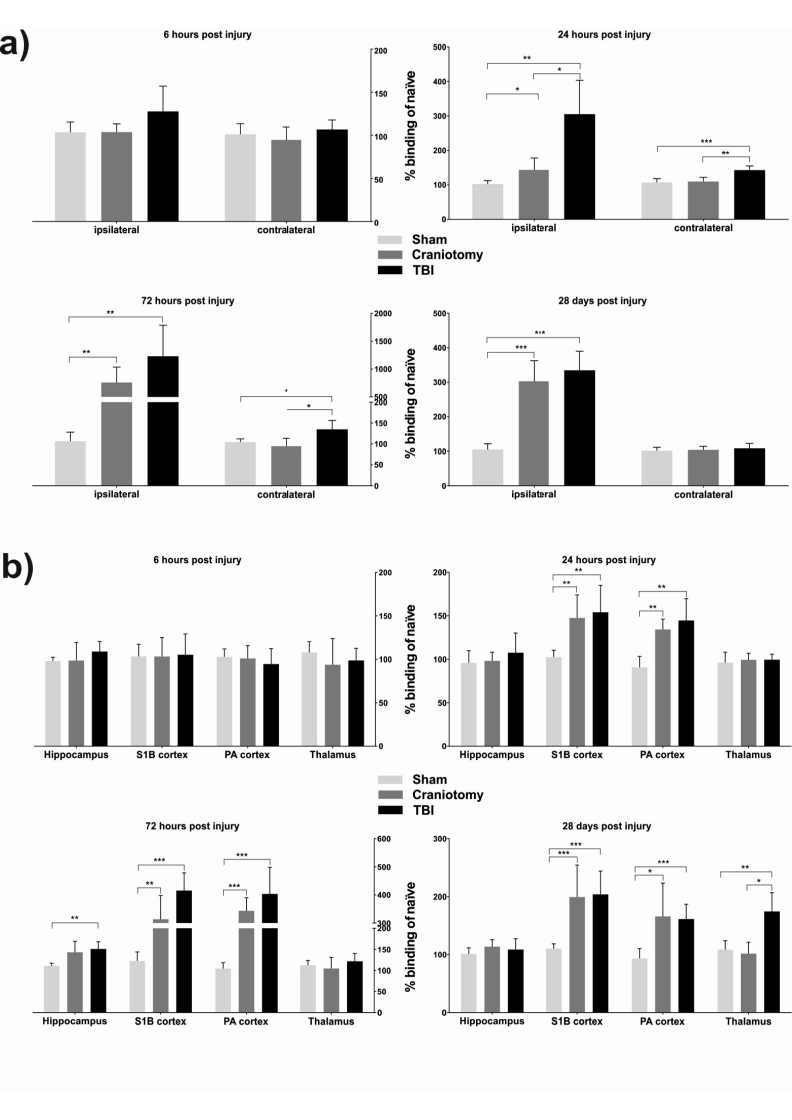
a)
6 hours post injury
24 hours post injury
72 hours post injury
28 days post injury
% binding of naïve
ipsilateral
contralateral
Sham
Craniotomy
TBI
b)
Hippocampus
S1B cortex
PA cortex
Thalamus

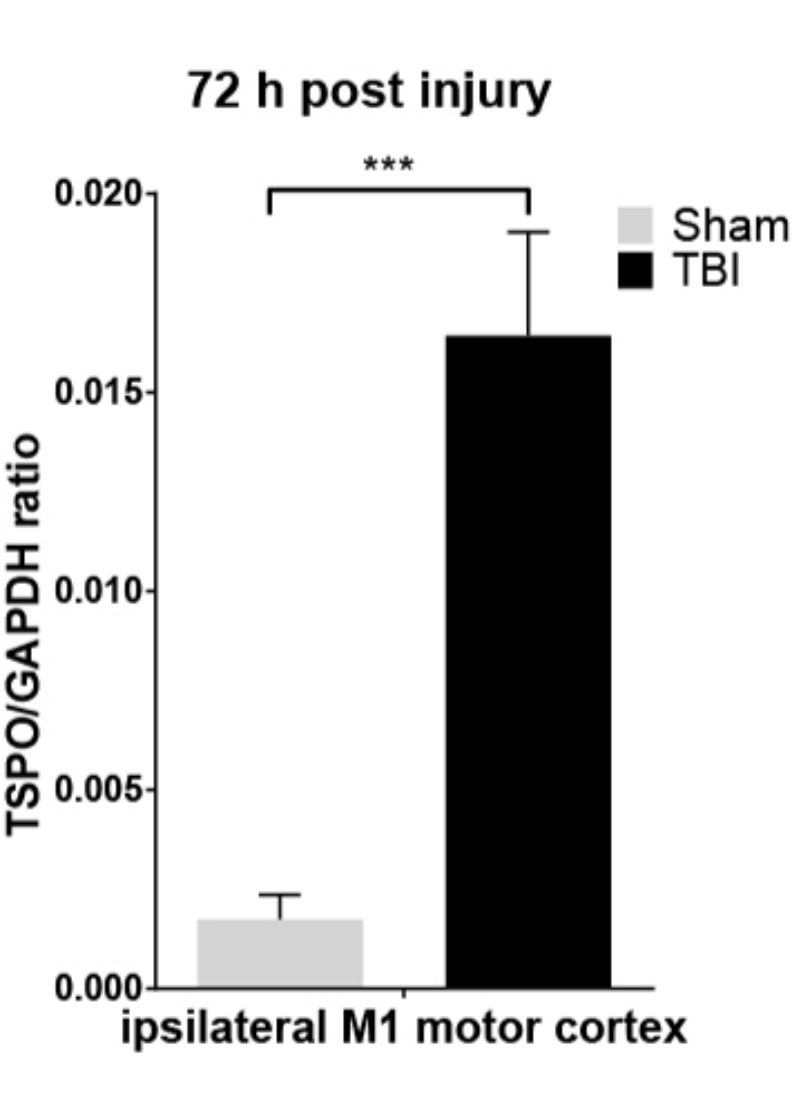
72 h post injury
***
0.020
0.015
0.010
0.005
0.000
TSPO/GAPDH ratio
Sham
TBI
ipsilateral M1 motor cortex

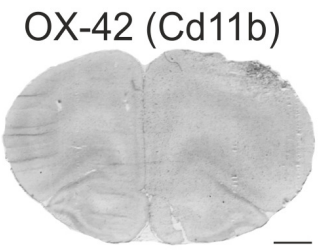
OX-42 (Cd11b)

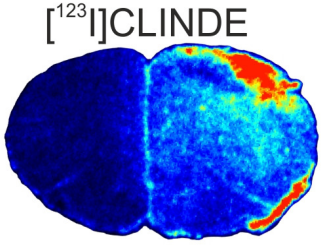
[123I]CLINDE

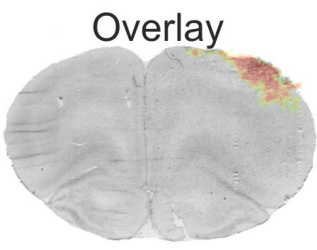
Overlay